



This is a repository copy of *Adaptive and sensitive fibre-optic fluorimetric transducer for air- and water-borne analytes*.

White Rose Research Online URL for this paper:  
<http://eprints.whiterose.ac.uk/142737/>

Version: Accepted Version

---

**Article:**

Alshammari, A.H., Kirwa, A. [orcid.org/0000-0002-7115-8919](https://orcid.org/0000-0002-7115-8919), Dunbar, A. [orcid.org/0000-0002-2313-4234](https://orcid.org/0000-0002-2313-4234) et al. (1 more author) (2019) Adaptive and sensitive fibre-optic fluorimetric transducer for air- and water-borne analytes. *Talanta*, 199. pp. 40-45. ISSN 0039-9140

<https://doi.org/10.1016/j.talanta.2019.02.055>

---

Article available under the terms of the CC-BY-NC-ND licence (<https://creativecommons.org/licenses/by-nc-nd/4.0/>).

**Reuse**

This article is distributed under the terms of the Creative Commons Attribution-NonCommercial-NoDerivs (CC BY-NC-ND) licence. This licence only allows you to download this work and share it with others as long as you credit the authors, but you can't change the article in any way or use it commercially. More information and the full terms of the licence here: <https://creativecommons.org/licenses/>

**Takedown**

If you consider content in White Rose Research Online to be in breach of UK law, please notify us by emailing [eprints@whiterose.ac.uk](mailto:eprints@whiterose.ac.uk) including the URL of the record and the reason for the withdrawal request.



[eprints@whiterose.ac.uk](mailto:eprints@whiterose.ac.uk)  
<https://eprints.whiterose.ac.uk/>

## Adaptive and sensitive fibre-optic fluorimetric transducer for air- and water-borne analytes

Alhulw H Alshammari<sup>\*a,d</sup>, Abraham Kirwa<sup>a,c</sup>, Alan Dunbar<sup>b</sup>, Martin Grell<sup>a</sup>

<sup>a</sup> Physics and Astronomy, University of Sheffield, Hicks Building, Hounsfield Rd, Sheffield S3 7RH, UK

<sup>b</sup> Chemical and Biological Engineering, The University of Sheffield, Mappin St, Sheffield S1 3JD, UK

<sup>c</sup> Department of Physical Sciences, Chuka University, P.O. Box 109-60400, Chuka, Kenya.

<sup>d</sup> College of Science, Aljouf University, Airport ST, Sakaka 72388, Saudi Arabia

**Keywords:** Sensor, Fibre optics, Lock in, DNT, MDMO-PPV.

\*Corresponding author, [ahfalshammari1@sheffield.ac.uk](mailto:ahfalshammari1@sheffield.ac.uk)

### Abstract

A sensitive fibre optic fluorescence intensity meter has been designed and built as a transducer to detect quenching of conjugated polymer fluorescence with minimum adjustment between air- and waterborne analytes. Only generic, commercially available parts including optical fibres, solvents, airbrush, standard optical and electronic parts, and a digital lock-in amplifier have been used, avoiding the need for a fluorescence spectrometer. To test the instrument, optical fibres were sensitised with the generic fluorescent poly(phenylene-vinylene) derivative MDMO-PPV and exposed to a variety of vapour pressures, and concentrations in water, of the nitroaromatic explosive 2,4 dinitrotoluene (DNT). We establish dimensionless Stern-Volmer constants ( $K_{SV}$ ) and limit-of-detection (LoD) for air- and water-borne DNT as  $K_{SV}(\text{air}) = 1.4 \times 10^7$  vs.  $K_{SV}(\text{water}) = 5.8 \times 10^6$  and  $\text{LoD}(\text{air}) = 10.9$  ppb and  $\text{LoD}(\text{water}) = 56$  ppb. These LoDs compare favourably to prior reports. We consider our study of the MDMO-PPV / DNT system as a successful test of our transducer design and recommend its wider use.

## 1. Introduction

In recent years, fibre optics have been used for a variety of applications beyond their original purpose in data communication. One of those is in the optical sensing of air- or water-borne target chemicals ('analytes'), where an analyte causes a change of optical absorption, or fluorescence, in a sensitiser, namely a 'chromophore' (absorption) or 'fluorophore' (fluorescence). Sometimes optical fibres are used to guide light to a sensitiser and/or pick up transmitted or fluorescent light to guide it to a spectrometer for detection [1, 2, 3]. It has become increasingly common though to use fibres directly as the substrate for the sensitiser, by stripping the fibre cladding from the core within a short section and then coating sensitiser directly onto the fibre core in that section. Such more direct use of fibre optics is favourable because of easy handling and fabrication, low cost and attenuation, flexibility, and can lead to high sensitivity [4, 5]. Fibres may detect the absorption of propagating fibre modes via their evanescent waves in the sensitised section [6, 7], or collect fluorescence of the sensitiser that has been excited by absorption of evanescent waves [1, 8, 9, 10, 11]. However, despite efforts such as fibre tapering and longer sensitised sections [4, 9, 10, 12], evanescent wave excited fluorometric sensors often suffer from low intensity. Alternatively, fluorescence may be excited by an external source and couple into a propagating fibre mode [4].

In this study, we adapt a lock-in based light detector that we have developed for an evanescent wave absorption sensor [6] as the transducer and systematically compare different fluorophore-sensitised fibre optic sensor operation modes. As an example analyte, we used the nitroaromatic explosive dinitrotoluene (DNT) both in vapour- and aqueous phase. As fluorophore, we used the fluorescent polymer poly(phenylene-vinylene) derivative poly[2-methoxy-5-(3',7'-dimethyloctyloxy)-1,4-phenylenevinylene] (MDMO-PPV) that is known to be quenched by trace amounts of nitroaromatic explosives dissolved in either water or organic solvents [13,14] albeit it has not previously been used for nitroaromatic vapour sensing. We here show that fibre- based MDMO-PPV sensors can be deployed for nitroaromatic sensing in both aqueous (waterborne) and vapour (airborne) phase with minimum adaptation between different phases. We compare and assess different excitation modes, and study the required response times and the photophysical degradation of the fluorophore. Photophysical degradation is rapid but we develop optimised operation procedures and 'baseline' experiments to account for it. Sensors require several minutes to equilibrate under airborne DNT, but respond much faster to waterborne DNT. We find a dimensionless Stern Volmer constant for the DNT/MDMO-PPV complex of  $K_{SV} = 1.14 \times 10^7$  for airborne DNT and  $K_{SV} = 5.8 \times 10^6$  for waterborne DNT. Limit-

of- detection (LoD) for airborne DNT is 10.9 ppb and 55.7 ppb for waterborne DNT. Our transducer compares favourably to alternative systems using PPV fluorophores for the detection of nitroaromatic vapours [15] and solutions [16, 2], and we propose to adopt it more widely for fluorimetric sensing.

## 2. Experimental

To prepare sensitised fibres, first a 30 cm length of multimode optical fibre (FT800UMT, Thorlabs), with a silica core of diameter 800  $\mu\text{m}$  with a 30  $\mu\text{m}$  thick transparent polymer cladding was cut from a fibre reel. The fibre's refractive indices of core and cladding, are 1.46 and 1.40 respectively, leading to 0.39 numerical aperture (NA) and  $18^\circ$  acceptance angle in water, and  $24.5^\circ$  in air. The fibre was cleaved, polished, and a 1 cm long section of the silica core was exposed by stripping off the polymer cladding. The exposed core was cleaned and dried, as described previously in [6,17] but in this case with the exposed section near the end of the fibre instead of the middle to adapt to fluorescence- rather than absorbance- based sensing. A 1 mg/mL solution of MDMO-PPV (Sigma Aldrich) in dichloromethane was prepared by stirring for an hour at 50  $^\circ\text{C}$ . To sensitise fibres, the MDMO-PPV solution was then sprayed onto the stripped section of the fibre using a WilTec airbrush (WilTec, Königsbenden 28, DE-52249 Eschweiler, sourced via ManoMano; nozzle diameter 0.3 mm, air pressure 1.5 bar) and left to dry under ambient air before using it. To determine fluorescence intensity, fluorescence was excited from a blue (405 nm) LED (LED 405L, Thorlabs), matching the absorption band of MDMO-PPV, which was controlled via a rocker switch to control excitation time. The LED was driven in series with a 150  $\Omega$  resistor from an AC + DC voltage adder circuit, adding an 8.15 V DC bias to a 5.641 kHz AC signal of  $\pm 2.5$  V taken from the reference output of a digital lock-in amplifier (USB LockIn250, Anfatec). Fluorescence was usually excited only briefly for 3 s with longer 'dark' intervals between measurements to minimise photophysical degradation of the fluorophore. Excitation was in two different configurations, 'side illumination' and 'evanescent wave' excitation. For side illumination, the sensitised section of the fibre was excited by LED light (405 nm) from  $\sim 5$  mm distance under  $\sim 90^\circ$  angle. Resulting fluorescence partly coupled into the fibre and was detected at the end face. For evanescent wave excitation, LED light (405 nm) was coupled into the fibre from one end face and propagated within the fibre. In the sensitised section of the fibre, the evanescent wave of propagating 405 nm light excited fluorescence in the sensitiser that partly coupled back into the fibre. One face of the fibre projected fluorescence onto a Centronic OSD5-5T photodiode (PD) via a high-pass optical wavelength filter (LP02-488RU-

25, Semrock) with a cut-on wavelength of 488 nm that blocks exciting light from the 405 nm LED but allows light from the MDMO-PPV fluorescence band (onset around 550 nm in the solid state) to reach the PD. The resulting PD photocurrent is fed into the input of a current/voltage (i/v) converter with transimpedance gain of 100 k $\Omega$ . The voltage delivered by the i/v converter was linked into the measurement input of the lock-in, set to AC coupling with a 100-fold preamplification and a 1 s output filter to give a DC 'V<sub>out</sub>' reading in the mV range that is proportional to MDMO-PPV fluorescence intensity. V<sub>out</sub> was recorded vs. time on a PC running a bespoke LabVIEW routine. The setup is adapted from the fibre optic absorbance meter described in more detail in [6,17], omitting the beam splitter and reference signal path required for absorbance measurement.

To generate test vapours, an open bottle containing 250 mg of high explosive 2,4 dinitro toluene (DNT) was placed in a thermalised container. The container was thermalised with different media (air at different temperatures, ice bath, salt/ice mix) to (20.1 / 16.3 / 0 / -5 / -15) °C, respectively, as measured by a testo 925 digital thermometer, to establish saturated vapour pressures  $p_{\text{sat}}$  at different temperatures, at and below ambient temperature. The thermalised DNT container was purged with pressurised dry nitrogen carrier gas with a flow rate of 500 mL/min that was pre-cooled by running several coils of pipe through same cooling medium. Reducing the temperature of the source allowed generation of DNT concentrations down to very low levels. Resulting DNT concentration is expressed as a normalised partial pressure  $p$ , given as the ratio of DNT saturated vapour pressure to standard atmospheric air pressure,  $p = p_{\text{sat}}(T) / p_{\text{atm}}$ . Therein  $T$  is the temperature of the DNT source,  $p_{\text{sat}}(T)$  is the saturated vapour pressure of DNT at  $T$ , and  $p_{\text{atm}} = 101.325$  kPa.  $p$  is dimensionless and we express it in parts-per-billion (ppb). The temperature dependency of DNT saturated vapour pressure  $p_{\text{sat}}(T)$  was given by Pella [18]. We thus obtained DNT vapour concentrations  $p = (150 / 89.7 / 8.4 / 4.8 / 0.73)$  ppb, respectively, i.e. covering the range from ambient saturation (150 ppb at 20.1 °C) down to approximately a 200-fold dilution. To realise an extremely low vapour pressure, we used picric acid (PA) instead of DNT. Picric acid (PA) is another nitroaromatic explosive but shows much lower vapour pressure than DNT, 0.028 parts-per-trillion (ppt) at ambient temperature [19]. Also, as a control experiment, we generated a saturated vapour of a non-nitrated aromatic, toluene, at ambient temperature, equal to 29.6 parts-per-thousand (ppt) [20]. The resulting vapours were delivered into a closed fibre optic test chamber (31 mL volume) held at ambient temperature via short tubes (to minimise parasitic condensation) with a similar

exhaust tube leading into a fume extractor funnel. The test chamber is hence purged within 4 seconds. Our system for detection of airborne DNT is illustrated in Fig. 1.

To prepare aqueous solutions of DNT, a stock solution was prepared by stirring 1 mg of DNT crystals in 1 ml of deionized water for a week using teflon magnetic bar under 22 °C, resulting in a saturated solution of 1.03 mM concentration [21]. To allow direct comparison with partial pressures of airborne DNT, we here express solution concentrations in the same dimensionless format as partial pressures. Given that 1L of water equals 55.6 mole, we can equate 1.03 mM = 18.5 parts- per- million (ppm). The stock solution was filtered by PTFE syringe mounted filters and transferred into a clean vial. 53.7  $\mu$ L aliquots of 18.5 ppm DNT stock solution were then pipetted repeatedly into a vessel holding 11 mL DI water, leading to DNT concentrations of (90, 180, 270, 360, 450, 540, 630, 720) ppb. For waterborne DNT detection, we modified the shown in Fig. 1. Instead of a test chamber, we used a vessel to hold DI water or DNT solution. Fluorescence excitation and detection remained the same.

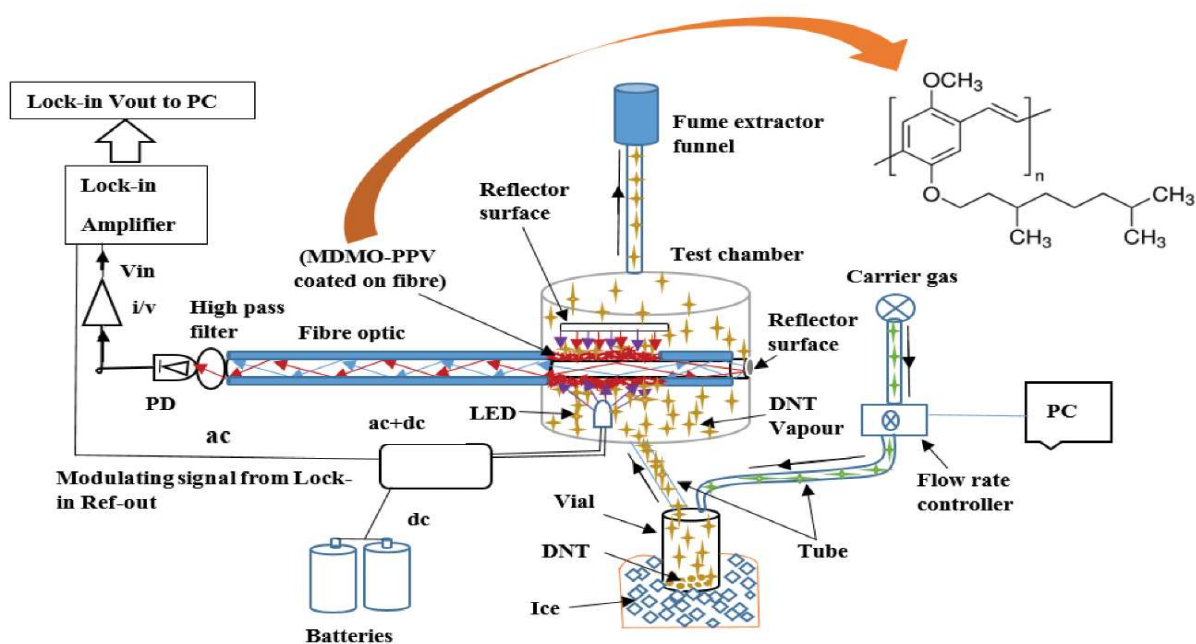


**Fig. 1** Schematic diagram of our sensor design and test vapour generator. Here, the ‘side illumination’ excitation mode is illustrated. Arrow: Chemical structure of MDMO-PPV.

### 3. Results and discussion

#### 3.1 Comparing side illumination and evanescent wave illumination

Fig. 2 shows lock-in output voltage  $V_{out}$  vs. time of two different fibres coated with MDMO-PPV, both excited by the same 405 nm LED. One fibre (shown black) was excited by the

evanescent wave of 405 nm light propagating within the fibre, the other (shown red) was excited externally from the side under  $\sim 90^\circ$  angle. There was no exposure to DNT vapours.

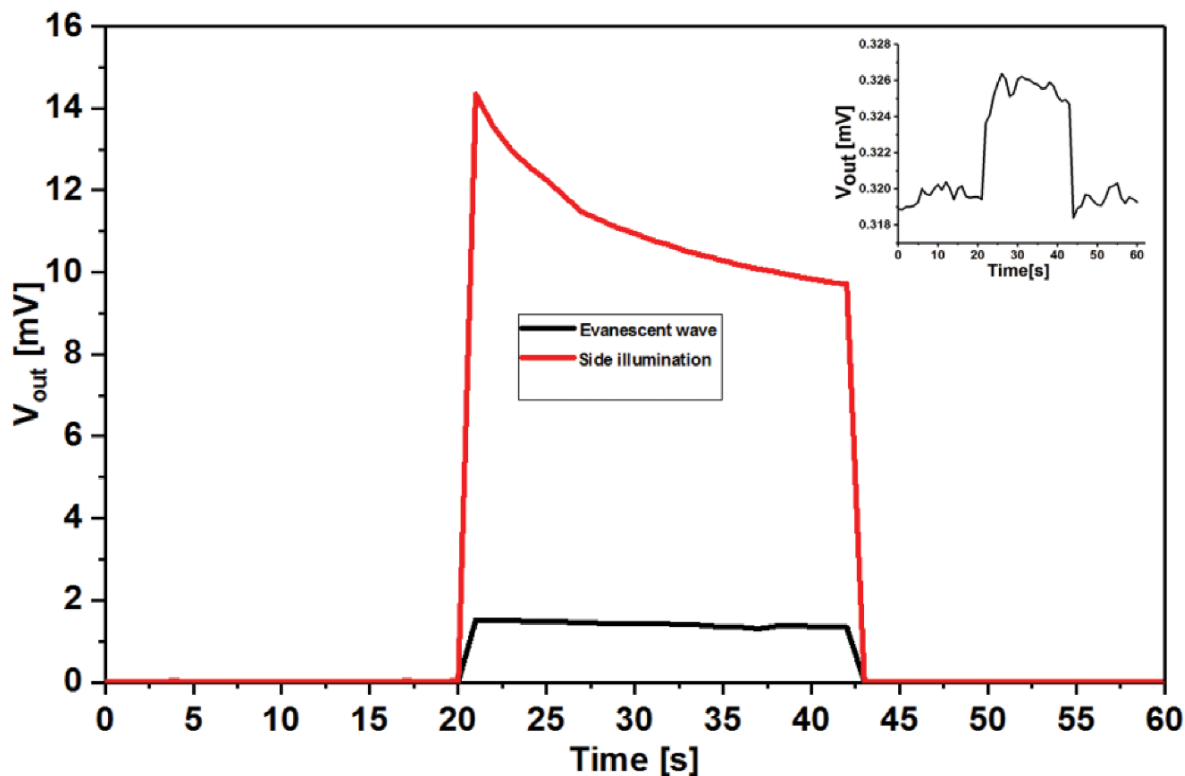


**Fig. 2:** Comparison between fluorescence intensity emitted from MDMO-PPV (405 nm excitation) under evanescent wave excitation (black) and side illumination (red). Excitation was turned on at 20 s and turned off at 45 s. The inset shows the intensity recorded from an unsensitised fibre under side illumination, which was turned on between 22s and 45s, without a high pass optical filter.

Detected fluorescence intensity is far higher for side illumination than for evanescent wave excitation. Evanescent wave excitation requires absorption of evanescent waves which is weaker than absorption under side illumination. While coupling- in of fluorescence from side illumination into the fibre is strong, the inset shows that direct coupling- in of exciting light into a stripped but non-sensitised fibre is very weak, 3 orders of magnitude weaker than fluorescence intensity. This is because side excitation under  $90^\circ$  is far outside the  $18^\circ$  ‘coupling cone’ given by the fibre’s numerical aperture (NA), while fluorescence is emitted under all angles, including those that can couple into propagating modes inside the fibre. Evanescent wave excitation requires an optical high pass filter to stop exciting light reaching the detector, but as we find here, it is not necessary under side illumination albeit we did keep it in our set-

up (it was only removed to record the inset to Fig. 2). Fig. 2 also shows that MDMO-PPV fluorescence intensity quickly degrades under illumination, particularly under side illumination. For the following sensing experiments, we have therefore worked with side illumination for a stronger signal, but limited excitation to 3 s ‘interrogation’ periods with extended dark intervals between interrogations to minimise photophysical degradation. We have also carried out degradation experiments in the absence of analyte to account for degradation.

### 3.2 Detecting airborne DNT vapours

Fig. 3 shows recorded values for lock-in output voltage vs. time at different DNT vapour concentrations,  $p$ ,  $V_{out}(t, p)$ , including a control experiment in a DNT- free atmosphere. For comparison, results for a fibre non- sensitised with MDMO-PPV are also shown.

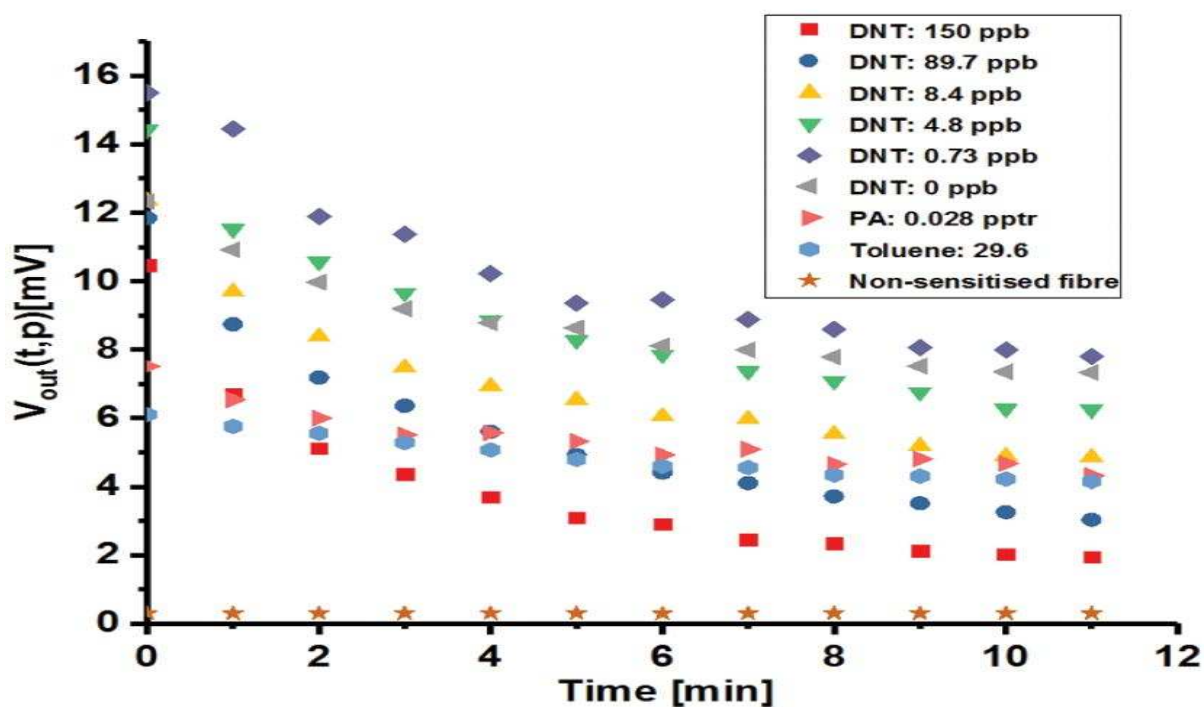


**Fig. 3:** Lock-in voltage output  $V_{out}(t,p)$  as a measure of fluorescence intensity for several MDMO-PPV sensitised optical fibres under blue LED excitation shown against time after starting the exposure to DNT at  $t = 0$  at different dimensionless vapour pressures,  $p$ . The fibres were illuminated and fluorescence was detected for 3 s once every minute. The non-sensitised fibre gives near-zero  $V_{out}$ .

The non-sensitised fibre shows near-zero  $V_{out}(t,0)$ , confirming that exciting light does not significantly couple into the fibre under side illumination. For all sensitised fibres at first 3 s

‘interrogation’, the recorded  $V_{out}$  for all DNT partial pressures  $p$ ,  $V_{out}(0,p)$ , was in the range (10.5 ... 15.5) mV, with some variation between fibres. Also, even at zero DNT pressure, recorded  $V_{out}(t,0)$  decays slightly with every interrogation, even though there can be no DNT-induced quenching. This indicates some photophysical degradation of MDMO-PPV even under brief excitation, which underscores the need to keep the excitation time as short as possible. Further, the measured value for  $V_{out}(t,p)$  is proportional to the number of fluorescence- active MDMO-PPV units, while our interest is focussed on the fluorescence-inactive units, as it is the quenched (inactive) rather than active units that indicate presence of DNT (‘on- to- off’).

Hence, for further analysis, all recorded values for  $V_{out}(t,p)$  were normalised and processed into a ‘fluorescence quenching response’  $FQR(t,p)$  [22] to account for these factors: First, all  $V_{out}(t,p)$  data were normalised to their initial values  $V_{out}(0,p)$ . Then they were multiplied by  $V_{out}(0,0) / V_{out}(t,0)$  to account for photodegradation unrelated to DNT, and finally subtracted from 1 to convert from a measure of active fluorophores into a measure of quenched fluorophores. In summary,  $FQR(t,p)$  represents the ratio of DNT- complexed vs. total MDMO-PPV fluorescent units and is calculated from  $V_{out}(t,p)$  by:

$$FQR(t,p) = 1 - [(V_{out}(t,p) / V_{out}(0,p)) \times (V_{out}(0,0) / V_{out}(t,0))] \quad (\text{eq. 1})$$

$FQR(t,p)$  ranges from zero (no quenching) to 1 (complete quenching). For ‘off- to- on’ fluorescence sensors, data would have to be analysed without the subtraction from 1. The resulting  $FQR(t,p)$  calculated from the  $V_{out}$  data shown in Fig. 3 via eq. 1 are shown in Fig. 4. Other researchers found curves of similar shape and timescale, e.g. [9, 22, 23].

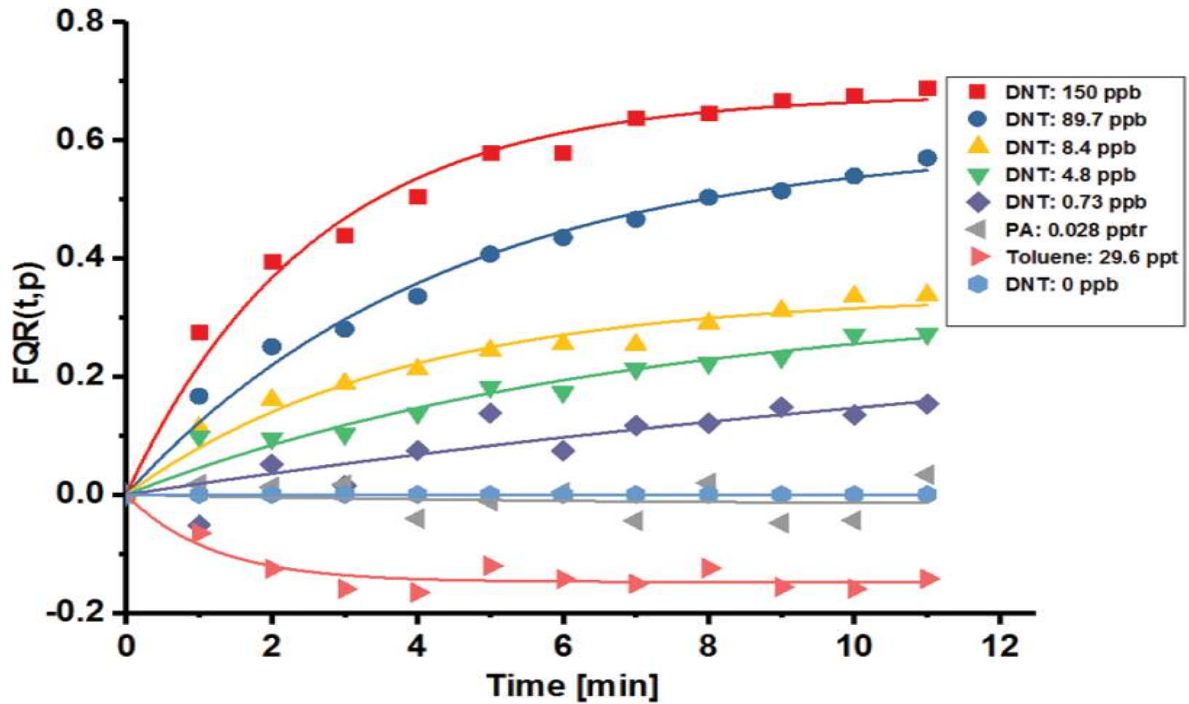


**Fig. 4:** Fluorescence quenching ratios  $FQR(t,p)$  calculated from the data in Fig. 3 with the help of eq. 1. Solid lines are fits to eq. 2 using Origin software.

By construction,  $FQR(t,0)$  remains zero at all times, reflecting the absence of DNT- induced quenching in the absence of DNT. All  $FQR(t,p)$  data under DNT show an initial increase over time, steeper for higher  $p$ , which after a few minutes approaches a final equilibrium value,  $FQR(\infty,p)$ , that increases with increasing  $p$ . This approach to equilibrium was fitted with an exponential model, eq. 2:

$$FQR(t,p) = FQR(\infty,p)[1 - \exp(-t / \tau(p))] \quad (\text{eq. 2})$$

With two fit parameters, an equilibrium value  $FQR(\infty,p)$  that is approached with a time constant,  $\tau(p)$ . The model provides good fits, shown as solid lines in Fig. 4. The fit parameters are summarised in table 1.

**Table 1:** Fit parameters, with errors, for  $FQR(t,p)$  shown in Fig. 4 when fitted to eq. 2 using Origin software. For some concentrations the experiment was repeated on a different fibre, repeat results shown in brackets.

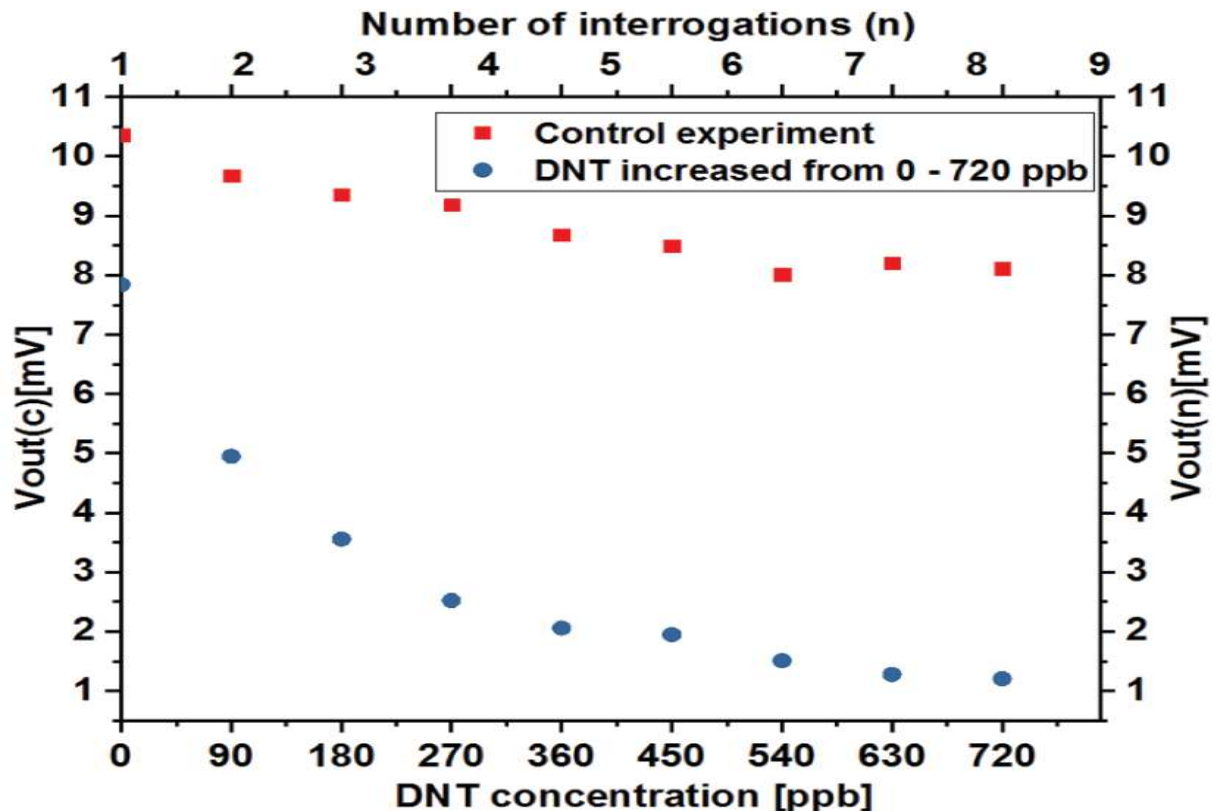
p [ppb]	FQR( $\infty$ ,p)	$\tau$ (p)[min]
0.73	0.10 +/- 0.01	2.4 +/- 1.2
4.8	0.31 +/- 0.04 [0.34 +/- 0.01]	5.9 +/- 1.5 [8.2 +/- 3.9]
8.4	0.34 +/- 0.02 [0.31 +/- 0.02]	3.6 +/- 0.6 [1.7 +/- 0.4]
89.7	0.60 +/- 0.02 [0.57 +/- 0.02]	4.3 +/- 0.4 [3.3 +/- 0.3]
150	0.68 +/- 0.01	2.6 +/- 0.2

Table 1 includes some fit parameters shown in brackets which were extracted from repeating experiments under (89.7 / 8.4 / 4.8) ppb DNT with another fresh fibre as shown in Fig. S1. Fibres that had been used in an exposure experiment did recover 85% of their initial fluorescence intensity after 40 hrs storage under dynamic vacuum at 50 °C, similar as it was observed for other fluorescent nitroaromatic explosive sensors previously [23]. This suggests that the fluorophore/nitroaromatic complex is slowly reversible, but not the photodegradation that is independent of complexation. We therefore conducted all experiments with freshly prepared fibres only, so that every curve in Fig. 3 was taken on a different fibre.

### 3.3 Detecting waterborne DNT

Same optical fibres and transducer can also be used for the detection of waterborne DNT with minimum adaptation, cf. experimental section. We now find that when we add DNT stock solution to water, the fluorescence response to increased DNT concentration is very fast and complete within 120 seconds, as shown in Fig. S2. This allows for a simpler calibration procedure where a single fibre is measured repeatedly while it is titrated with DNT in concentration (c) increments of 90 ppb added in 2 minute intervals. Due to the fast equilibration, measured  $V_{out}(t = 2 \text{ minutes}, c)$  can be taken as  $V_{out}(t \rightarrow \infty, c)$  and is simply reported as  $V_{out}(c)$ .

Note we annotate waterborne concentrations as ‘c’ to distinguish from partial pressures, p, of the airborne analyte, but report both as dimensionless fractions, ppm or ppb, relative to the respective carrier medium. However, there again is a decay of fluorescence intensity due to photodegradation with every 3 second fibre ‘interrogation’. This is again accounted for by a control experiment where a (different) fibre was repeatedly interrogated in same 2 minute intervals in DI water, without DNT titration. Results are shown in Fig. 5.



**Fig. 5:** Lock-in voltage output  $V_{out}(c)$  (blue circles) as a measure of fluorescence intensity for MDMO-PPV sensitised optical fibre under blue LED excitation shown against DNT concentration in water from 0 - 720 ppb. Also shown, a control experiment (red squares), vs. a number of interrogation periods.

The resulting fluorescence quenching ratio  $FQR(c)$  for waterborne DNT, which corresponds to  $FQR(\infty,p)$  for airborne DNT, is calculated from data in Fig. 5 using eq. 3:

$$FQR(c) = 1 - \left[ \left( \frac{V_{out}(c)}{V_{out}(c=0)} \right) \times \left( \frac{V_{out}(n=1)}{V_{out}(n)} \right) \right] \quad (\text{eq. 3})$$

Note how the second factor on the right- hand side compensates for photodegradation that is independent of DNT concentration, similar as in eq. 1. Resulting FQR(c) is tabulated in table 2:

**Table 2:** FQR(c) vs c for waterborne DNT.

<b>c [ppb]</b>	<b>FQR(c)</b>
90	0.32
180	0.50
270	0.64
360	0.69
450	0.70
540	0.75
630	0.79
720	0.80

### 3.4 Discussion: airborne DNT vapours

The time constants  $\tau$  required to reach equilibrium FQR( $\infty$ ,p) are in the order of a few minutes with no systematic variation with p, significantly longer than the 4 seconds required to purge the 31 mL sample chamber by a stream of 500 mL/minute flow of test vapour. This observation is consistent with a ‘static’ quenching process [e.g. 24] where DNT vapour first diffuses into the MDMO-PPV fibre coating to form fluorophore/DNT complexes that then quench excitons when excited by LED illumination. A ‘dynamic’ quenching process would instead rely on the collision of a DNT molecule with a previously uncomplexed fluorophore while this is in the excited state; this would not need minutes to build- up. We therefore, believe  $\tau$  represents the time for analyte to diffuse into the MDMO-PPV film coated onto the fibre, which does not

depend on  $p$ , but does somewhat vary with variations in MDMO-PPV coating resulting from the spraying process.  $\tau$  is long because the density of the airborne phase is low.

On the other hand, the equilibrium value of fluorescence quenching response  $FQR(\infty, p)$  does systematically depend on DNT concentration, i.e. dimensionless partial pressure  $p$ . Qualitatively, Fig. 4 shows that at the lowest DNT concentration used here of  $p = 0.73$  ppb we still find FQR above noise. This is at  $\approx 200$ - fold dilution of the saturated vapour pressure at ambient temperature, using only a generic fluorescent polymer, albeit formal analysis of LoD returns a higher value. Under the extremely low (saturated) vapour pressure of picric acid (0.028 ppb), no clear response can be found though.

For quantitative analysis, we present response in a Stern- Volmer (SV) plot, Fig. 6. In the SV plot, fluorescence quenching is expressed as  $I(p)/I(0) - 1 = I/I_0 - 1$ ; this is related to  $FQR(\infty, p)$  by  $I_0/I - 1 = FQR(\infty, p) / [1 - FQR(\infty, p)]$ .

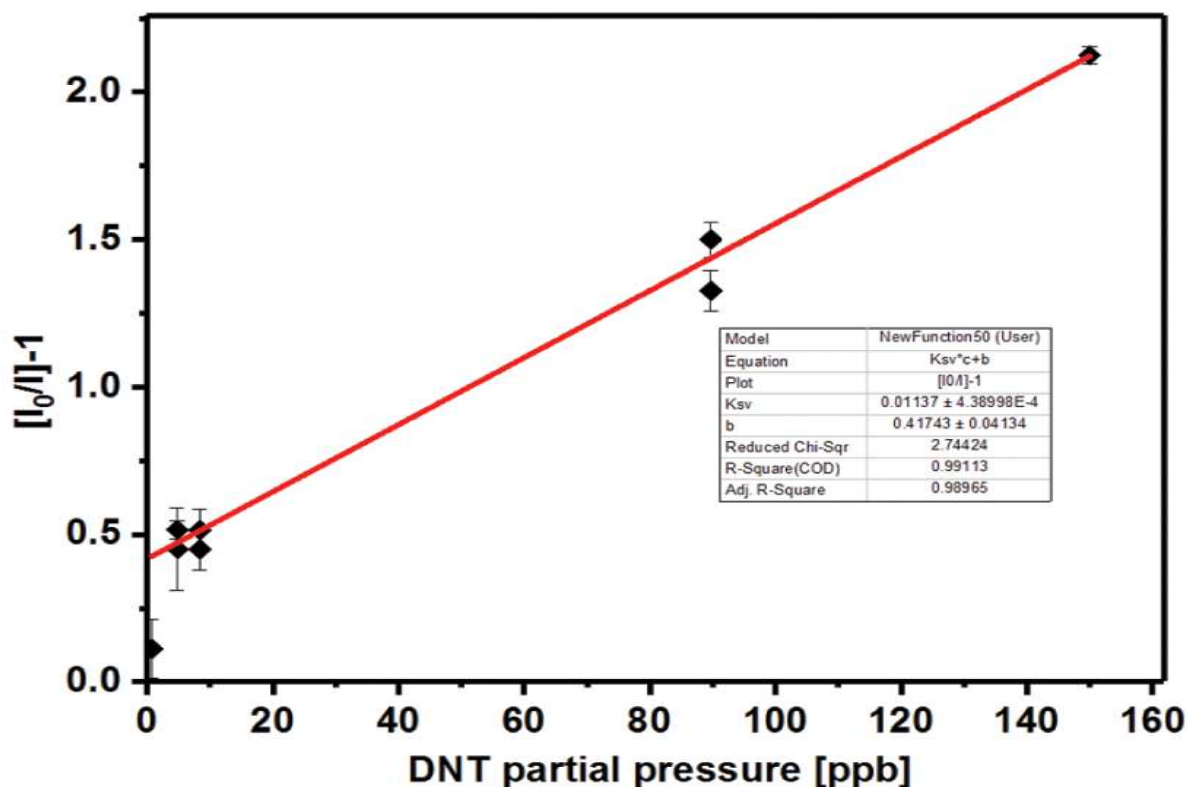


**Fig. 6.** Stern-Volmer plot for quenching of MDMO-PPV fluorescence by airborne DNT in the concentration range (0-150) ppb. Data from table 1.

A straight line is fitted with intercept and find  $b \pm \Delta b$  which gives DNT / MDMO-PPV Stern Volmer constant,  $K_{SV}$ , as its slope.  $K_{SV}$  quantifies the strength of analyte / sensitiser interaction relative to analyte / carrier medium interaction. Fitting the straight line slope in Fig. 6 gives  $K_{SV} = (1.14 \pm 0.00044) \times 10^7$ . Note  $K_{SV}$  is dimensionless as it is evaluated from dimensionless partial pressure, however, since  $p$  is expressed as ppb ( $10^{-9}$ ),  $K_{SV}$  is  $10^9$  times the value of the slope in a plot vs.  $1/p$  (in ppb).  $K_{SV}$  defines a characteristic vapour pressure  $p_{1/2} = 1/K_{SV} = 88$  ppb where  $FQR(\infty, p) = 1/2$ . The fit in Fig. 6 also gives an intercept ( $b$ ) with error  $\Delta b$ , and we calculate a limit- of- detection (LoD) by the common ‘3 errors’ criterion,

$$\text{LoD} = 3\Delta b / K_{SV} \quad (\text{eq.4})$$

Which here leads to  $\text{LoD} = 10.9$  ppb for the detection of airborne DNT. Note however that the plot does not give zero intercept ( $b$ ) as expected, so the SV relation is not a good fit at very low  $p$ . This accounts for the formally evaluated LoD of 10.9 ppb being rather larger than the clearly visible response to 0.73 ppb in Fig. 4. Nevertheless, our LoD compares favourably to LoD of 30 ppb reported in [15] for detection of DNT with similar PPV polymer and a conventional spectrometer.

PPV based polymers generally are sensitive to several nitroaromatic explosive vapours. However, selectivity between different nitroaromatics is not practically desirable, as all of them should be detected. We have therefore not investigated it here, instead we made sure MDMO-PPV is selective between nitroaromatics and their non- nitrated analogue, toluene. Despite toluene’s much higher vapour pressure (saturated vapour pressure 29.6 parts- per- thousand (ppt) at ambient temperature [20]), it elicits no fluorescence quenching in MDMO-PPV, cf Fig. 4. Fluorescence intensity is in fact enhanced (formally expressed as negative FQR) under toluene vapour, which agrees with the known property of PPV polymers that they are highly fluorescent in organic solvents [25], even brighter than in solid films, due to separation of fluorophores from mutual interactions. Sensing is hence not compromised by a response to interferants.

### 3.5 Discussion: waterborne DNT

As we show in supporting information (Fig. S2), fibres respond to waterborne DNT much faster than for airborne DNT. We assign this to the higher density of the carrier medium. Note, concentrations are given as molar fractions (or partial pressures for airborne DNT, which is

equivalent to molar fraction). For any given molar fraction, the density of analyte measured per unit volume is far larger in the denser liquid carrier medium than in the vapour phase, leading to a quicker supply of DNT to the fluorophore.

Fig. 5 shows a clear quenching response even under 90 ppb waterborne DNT, going far beyond the photophysical degradation under interrogation in the absence of DNT. This indicates a LoD significantly below 90 ppb. The photodegradation- compensated FQR(c) data (table 2) are again presented in the Stern- Volmer plot, Fig. S3. We now find a straight- line fit with near-zero intercept (b), indicating full agreement with Stern Volmer law, albeit we have not explored extremely low concentrations ( $c \ll 1/K_{SV}$ ) as in gas sensing. Stern Volmer constant  $K_{SV}$  is now  $K_{SV} = (5.8 \pm 0.00025) \times 10^6$ , again in dimensionless format, less than half as in the vapour phase. As  $K_{SV}$  quantifies analyte / sensitiser interaction relative to analyte / carrier medium interaction, the smaller  $K_{SV}$  shows that it is harder for the sensitiser to extract DNT from water than from air as the aqueous carrier medium provides better solvation. The LoD is evaluated in the same way as for airborne DNT, LoD = 56 ppb for the detection of waterborne DNT, less than half as reported in [16].

#### 4. Conclusions

We have developed a fibre optic transducer with lock- in detection for fluorimetry that can be adapted easily for sensing either air- or waterborne analytes. Our transducer requires no optical spectrometer. We establish ‘side illumination’ as superior to evanescent- wave excitation of fluorescence. The easy adaptation between sensing in air or water allows us to compare the sensing performance of sensitiser/analyte systems between different carrier media. We investigate this on the example of the nitroaromatic explosive DNT detected by the fluorescent polymer MDMO-PPV, which previously had only been reported in water [13]. In both media, MDMO-PPV fluorescence rapidly decays over time even in the absence of analyte. We minimise this by limiting read- out to short excitation intervals, separated by extended ‘dark’ periods. We also show how to account for the remaining degradation. Response is significantly faster for waterborne than for airborne analyte, which we explain by the higher density of the liquid vs. the gaseous medium. Many previous reports on fluorescence- based detection of explosive vapours tested under saturation pressure at ambient temperature only [8-9, 26, 27], which does not allow to establish Stern Volmer constant ( $K_{SV}$ ) or limit- of- detection (LoD), and is unrealistic in practical situations where sources may be distant or concealed. Here, we explored a range of analyte concentrations, expressed in dimensionless (parts- per- billion)

format. For the same MDMO-PPV / DNT sensitiser / analyte system, the Stern Volmer constant for fluorescence quenching is larger for airborne rather than waterborne analyte,  $K_{SV}(\text{air}) \sim 1.4 \times 10^7$  vs.  $K_{SV}(\text{water}) \sim 5.8 \times 10^6$ . This indicates better solvation of analyte in water vs. air. We found LoD of 10.9 ppb in air and 56 ppb in water which are  $\sim 2.7$  times below previously reported LoDs for DNT sensing with PPV derivatives [15,16]. We consider our study of the MDMO-PPV / DNT system as a successful test of our transducer design and recommend its wider use for other sensitiser / analyte systems.

### Acknowledgements

Alhulw H Alshammari is grateful to the Cultural Attaché of Saudi Arabia to the UK and Aljouf University, Saudi Arabia, for providing him with a fellowship for his PhD studies. Abraham Kirwa thanks the Commonwealth Commission for providing a PhD fellowship, reference KECS-2014-277.

### References

- [1] Z. Wang, Z.Y. Wang, J. Ma, W.J. Bock, D. Ma, Effect of film thickness, blending and undercoating on optical detection of nitroaromatics using fluorescent polymer films, *Polymer (Guildf)*. 51 (2010) 842–847. <https://doi.org/10.1016/j.polymer.2010.01.003>.
- [2] F. Chu, G. Tsiminis, N.A. Spooner, T.M. Monro, Explosives detection by fluorescence quenching of conjugated polymers in suspended core optical fibers, *Sensors Actuators B. Chem.* 199 (2014) 22–26. <https://doi.org/10.1016/j.snb.2014.03.031>.
- [3] S. Ruan, H. Ebendorff-Heideprie, Y. Ruan, Optical fibre turn-on sensor for the detection of mercury based on immobilized fluorophore, *Measurement*. 121 (2018) 122–126. <https://doi.org/10.1016/j.measurement.2018.01.071>.
- [4] C. Pulido, Ó. Esteban, Improved fluorescence signal with tapered polymer optical fibers under side-illumination, *Sensors Actuators B. Chem.* 146 (2010) 190–194. <https://doi.org/10.1016/j.snb.2010.02.006>.

- [5] E. Rodríguez-Schwendtner, M.C. Navarrete, Ó. Esteban, N. Díaz-Herrera., A. González-Cano, Fluorescence excitation on tapered polymer optical fibers through microfiber evanescent field, 24th Int. Conf. Opt. Fibre Sensors. 9634 (2015) 96346D. <https://doi.org/10.1117/12.2193920>.
- [6] K.A. Tuwei, N.H. Williams, M. Grell, Fibre optic absorbance meter with low limit of detection for waterborne cations, *Sensors Actuators, B Chem.* 237 (2016) 1102–1107. <https://doi.org/10.1016/j.snb.2016.05.065>.
- [7] S. Chauhan, N. Punjabi, D. Sharma, S. Mukherji, Evanescent wave absorption based S-shaped fiber-optic biosensor for immunosensing applications, *Procedia Eng.* 168 (2016) 117–120. <https://doi.org/10.1016/j.proeng.2016.11.161>.
- [8] H.H. Nguyen, X. Li, N. Wang, Z.Y. Wang, J. Ma, W.J. Bock, D. Ma, Fiber-Optic Detection of Explosives Using Readily Available Fluorescent Polymers, *Macromolecules.* 42 (2009) 921–926. <https://doi.org/10.1021/ma802460q>.
- [9] F. Liu, M. Cui, J. Ma, G. Zou, Q. Zhang, An optical fiber taper fluorescent probe for detection of nitro-explosives based on tetraphenylethylene with aggregation-induced emission, *Opt. Fiber Technol.* 36 (2017) 98–104. <https://doi.org/10.1016/j.yofte.2017.03.004>.
- [10] F. Long, M. He, H.C. Shi, A.N. Zhu, Development of evanescent wave all-fiber immunosensor for environmental water analysis, *Biosens. Bioelectron.* 23 (2008) 952–958. <https://doi.org/10.1016/j.bios.2007.09.013>.
- [11] F. Long, C. Gao, H.C. Shi, M. He, A.N. Zhu, A.M. Klibanov, A.Z. Gu, Reusable evanescent wave DNA biosensor for rapid , highly sensitive , and selective detection of mercury ions, *Biosens. Bioelectron.* 26 (2011) 4018–4023. <https://doi.org/10.1016/j.bios.2011.03.022>.
- [12] G.P. Anderson, J.P. Golden, F.S. Ligler, An Evanescent Wave Biosensor- Part I: Fluorescent Signal Acquisition from Step-Etched Fiber Optic Probes, *IEEE Trans. Biomed. Eng.* 41 (1994) 578–584. <https://doi.org/10.1109/10.293245>.
- [13] M.D. Woodka, V.P. Schnee, M.P. Polcha, Fluorescent Polymer Sensor Array for Detection and Discrimination of Explosives in Water, *Anal. Chem.* 82 (2010) 9917–9924. <https://doi.org/10.1021/ac102504t>.
- [14] K. Saxena, P. Kumar, V.K. Jain, Fluorescence quenching studies of conjugated polymer poly[2-methoxy-5-(30,70-dimethyloctyloxy)-1,4-phenylenevinylene in the presence of TNT, *J. Lumin.* 130 (2010) 2260–2264. <https://doi.org/10.1016/j.jlumin.2010.07.001>.

- [15] R.N. Gillanders, I.D.W. Samuel, G.A. Turnbull, A low-cost , portable optical explosive-vapour sensor, *Sensors Actuators B. Chem.* 245 (2017) 334–340. <https://doi.org/10.1016/j.snb.2017.01.178>.
- [16] R.N. Gillanders, J.M.E. Glackin, I.A. Campbell, I.D.W. Samuel, G.A. Turnbull, Advances in Optical Sensing of Explosive Vapours, in: *Proc. 6th Int. Conf. Photonics, Opt. Laser Technol.*, SCITEPRESS - Science and Technology Publications, 2018: pp. 323–327. <https://doi.org/10.5220/0006729403230327>.
- [17] A.K. Tuwei, N.H. Williams, M.Y. Mulla, C. Di Natale, R. Paolesse, M. Grell, ‘Rough guide’ evanescent wave optrode for colorimetric metalloporphyrine sensors, *Talanta*. 164 (2017) 228–232. <https://doi.org/10.1016/j.talanta.2016.11.057>.
- [18] P.A. Pella., Measurement of the vapor pressures of TNT, 2,4-DNT, 2,6-DNT, and EGDN, *J.Chem.Thermodynamics*. 9 (1977) 301–305. [https://doi.org/10.1016/0021-9614\(77\)90049-0](https://doi.org/10.1016/0021-9614(77)90049-0).
- [19] R.B. Cundall, T.F. Palmer, C.E.C. Wood, Vapour pressure measurements on some organic high explosives, *J. Chem. Soc. Faraday Trans. 1 Phys. Chem. Condens. Phases*. 74 (1978) 1339–1345. <https://doi.org/10.1039/f19787401339>.
- [20] L.M. Besley, G.A. Bottomley, Vapour pressure of toluence from 273.15 to 298.15 K, *J. Chem. Thermodyn*. 6 (1974) 577–580. [https://doi.org/10.1016/0021-9614\(74\)90045-7](https://doi.org/10.1016/0021-9614(74)90045-7).
- [21] J.M. Phelan, J.L. Barnett, Solubility of 2,4-Dinitrotoluene and 2,4,6-Trinitrotoluene in Water, *J. Chem. Eng. Data*. 46 (2001) 375–376. <https://doi.org/10.1021/je000300w>.
- [22] K.R. Ghosh, S.K. Saha, Z.Y. Wang, Ultra-sensitive detection of explosives in solution and film as well as the development of thicker film effectiveness by tetraphenylethene moiety in AIE active fluorescent conjugated polymer, *Polym. Chem*. 5 (2014) 5638–5643. <https://doi.org/10.1039/c4py00673a>.
- [23] H. Ma, F. Li, Z. Zhang, M. Zhang, Rapid DNT fluorescent films detection with high sensitivity and selectivity, *Sensors Actuators, B Chem*. 244 (2017) 1080–1084. <https://doi.org/10.1016/j.snb.2017.01.098>.
- [24] G. He, N. Yan, J. Yang, H. Wang, L. Ding, S. Yin, Y. Fang, Pyrene-Containing Conjugated Polymer-Based Fluorescent Films for Highly Sensitive and Selective Sensing of TNT in Aqueous Medium, *Macromolecules*. 44 (2011) 4759–4766. <https://doi.org/10.1021/ma200953s>.
- [25] R.A. Abumosa, B.A. Al-Asbahi, M.S. AlSalhi, Optical properties and amplified spontaneous emission of novel MDMO-PPV/C500 hybrid, *Polymers (Basel)*. 9 (2017) 71. <https://doi.org/10.3390/polym9020071>.

[26] C.P. Chang, C.Y. Chao, J.H. Huang, A.K. Li, C.S. Hsu, M.S. Lin, B.R. Hsieh, A.C. Su, Fluorescent conjugated polymer films as TNT chemosensors, *Synth. Met.* 144 (2004) 297–301. <https://doi.org/10.1021/ja982293q>.

[27] H. Nie, Y. Zhao, M. Zhang, Y. Ma, M. Baumgarten, K. Müllen, Detection of TNT explosives with a new fluorescent conjugated polycarbazole polymer, *Chem. Commun.* 47 (2011) 1234–1236. <https://doi.org/10.1039/c0cc03659e>.

### Supplementary information.

In Fig. S1. we have repeated the airborne DNT sensing experiment with fresh fibres for each of the following DNT concentrations: (89.7 / 8.4 / 4.8) ppb. All remaining analysis and fitting have been carried out as for Fig. 3 and 4.

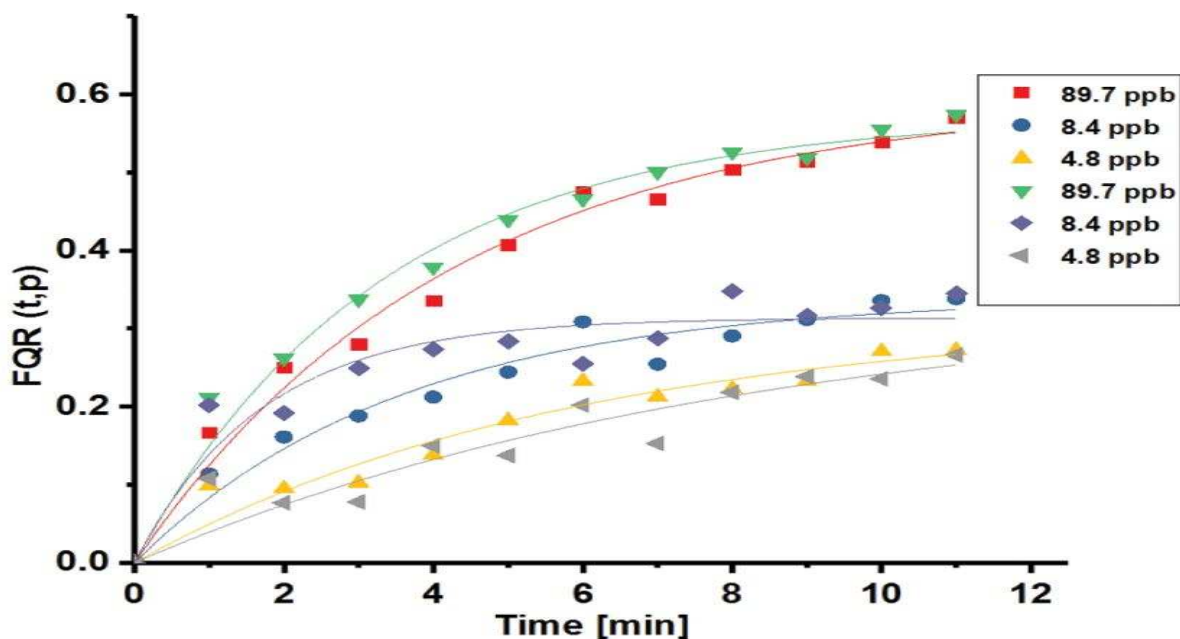


**Fig. S1:** Fluorescence quenching ratios  $FQR(t,p)$  calculated and fitted in a way same to Fig. 4.

In Fig. S2, we show the response characteristic of MDMO-PPV to 90 ppb DNT in water vs. time,  $FQR(c = 90\text{ppb}, t)$ . The exponential fit has a time constant of 33 s, significantly shorter than for airborne DNT.

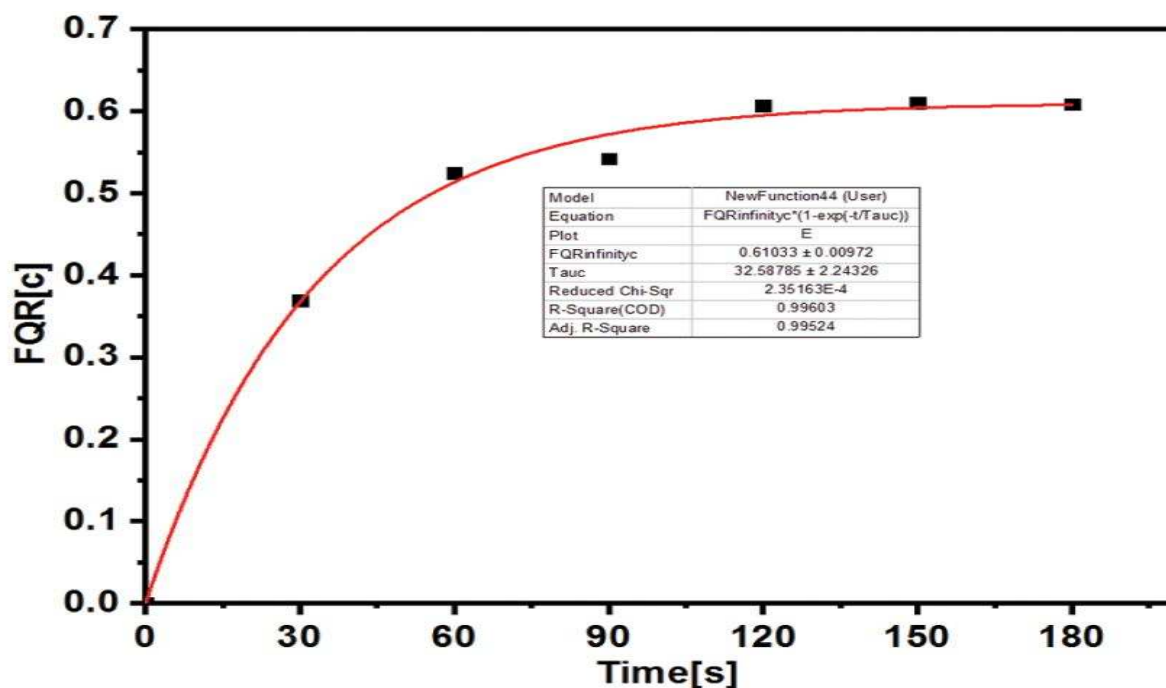


**Fig. S2:** Fluorescence quenching ratios  $FQR(t,c)$  under 90 ppb DNT concentration in water against time [seconds].

In Fig. S3, we show the Stern-Volmer plot for Different DNT concentrations (0-720 ppb) in DI-water by an increment of 90 ppb using same sensitised fibre.

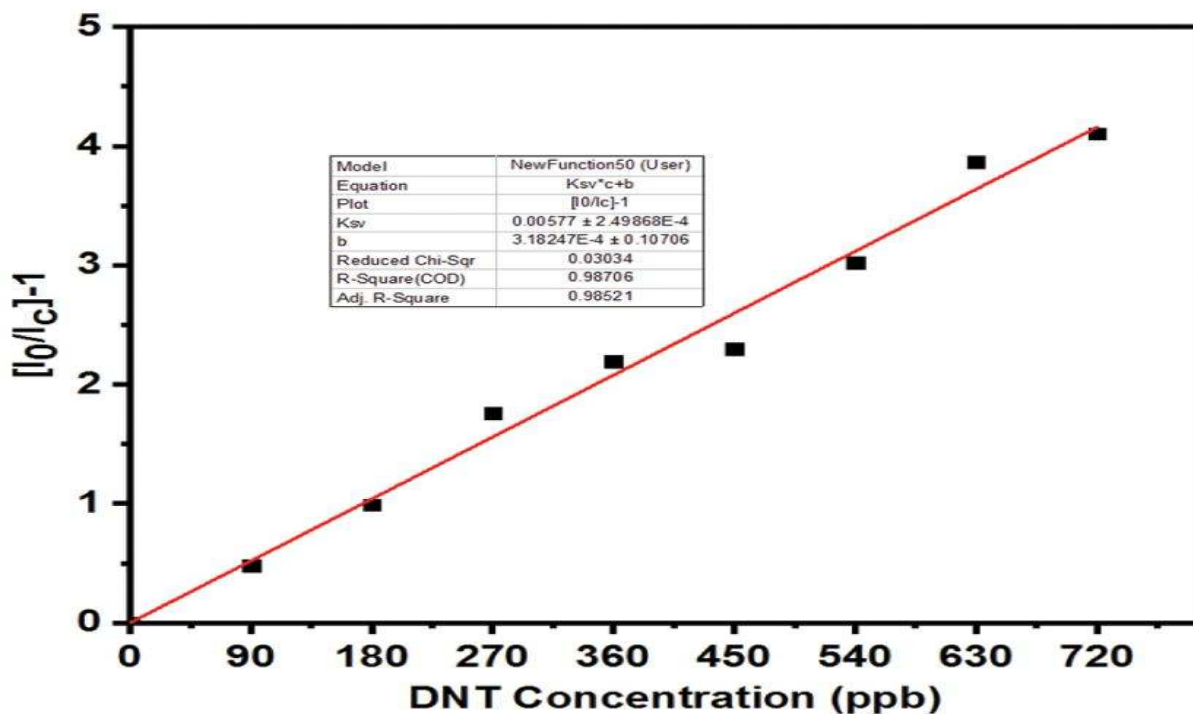


**Fig. S3:** Stern-Volmer plot for quenching of MDMO-PPV fluorescence by waterborne DNT in the concentration range (0-720 ppb). Data from table 2.

